Pakistan J. Zool., pp 1-11, 2026. **DOI**: https://dx.doi.org/10.17582/journal.pjz/20250630084225

DNA Methylation Biomarkers for Diagnosis of Breast Cancer: Focus on *FGFR1* and *FGF2*

Iqra Qadir[1], Faiza Inayat[2], Muhammad Akhtar Ali[1], John Lunec[3] and Naveed Shahzad[1]*

[1]*School of Biological Sciences, University of the Punjab, Lahore, Pakistan*
[2]*School of Biochemistry and Biotechnology. University of the Punjab, Lahore, Pakistan*
[3]*Biosciences Institute, Newcastle University Cancer Centre, United Kingdom*

Article Information
Received 30 June 2025
Revised 09 September 2025
Accepted 27 September 2025
Available online 25 May 2026
(early access)

Authors' Contribution
NS and JL designed the study. IQ performed lab experiments and wrote the manuscript. FI assisted in bioinformatics analysis, and MAA assisted with IHC interpretation. All authors approved the final manuscript.

Key words
Methylation, Expression, Breast Cancer, Epigenetics, Biomarkers

ABSTRACT

DNA methylation biomarkers offer promising avenues for the early detection of breast cancer (BC), especially in difficult-to-diagnose subtypes such as triple-negative breast cancer (TNBC). In this study, we investigated the methylation status and gene expression profiles of *FGFR1* and *FGF2* in a panel of 11 breast cancer cell lines and BC patient-derived tissues. Combined Bisulfite Restriction Analysis (COBRA), qPCR, Western blotting, immunohistochemistry (IHC), and bioinformatic analyses using TCGA data were employed. *FGFR1* and *FGF2* exhibited variable expression levels across luminal, HER2-enriched, and basal-like TNBC cell lines. Methylation at the promoter region of *FGF2* was detected in a limited subset (MCF7), while *FGFR1* showed minimal promoter methylation. A significant inverse correlation was observed between gene expression and methylation for both *FGFR1* and *FGF2*. IHC confirmed strong cytoplasmic expression of *FGFR1* and *FGF2* in tumour tissues compared to the normal counterpart. Furthermore, ROC analysis demonstrated high diagnostic accuracy for *FGFR1* (AUC = 0.88) and *FGF2* (AUC = 0.86). Bioinformatic analysis supported the clinical relevance of these markers, highlighting their prognostic significance and pathway enrichment in cancer progression. These findings underscore the potential of *FGFR1* and *FGF2* as epigenetic biomarkers for breast cancer detection and stratification.

INTRODUCTION

Breast cancer continues to be the most frequently diagnosed cancer in women globally, with approximately 2.5 million new cases and 720,000 deaths projected in 2025 (GLOBOCAN, 2024). This growing incidence highlights the urgent need for enhanced early detection strategies. Although molecular diagnostics have enhanced our ability to classify subtypes, triple-negative breast cancer (TNBC) remains particularly difficult to treat due to a lack of effective therapeutic targets.

Epigenetic mechanisms, especially DNA methylation, have emerged as key contributors to cancer development and progression. Hypermethylation in gene promoters often leads to the silencing of tumor suppressor genes, making this an attractive route for identifying novel biomarkers (Jones *et al*., 2023). DNA methylation assays offer distinct advantages, including chemical stability and compatibility with cell-free DNA (cfDNA), enabling non-invasive diagnostic applications (Luo *et al*., 2024). DNA methylation biomarkers offer distinct benefits over traditional RNA- or protein-based approaches. Their chemical robustness, detectability in minute DNA samples, and adaptability to various specimen types, including cfDNA and formalin-fixed tissues, make them highly promising (Heyn and Esteller, 2012). Numerous investigations have identified differentially methylated regions (DMRs) linked to breast cancer subtypes, stages, and outcomes (Manoochehri *et al*., 2022). Early work by Widschwendter and Jones (2002) highlighted unique methylation patterns in tumor versus normal tissue, a foundation furthered by recent high-throughput studies (Zhang *et al*., 2020; Luo *et al*., 2024).

FGFR1 and *FGF2* are pivotal to the FGF signaling axis, which governs cellular proliferation, migration, angiogenesis, and survival. Disruptions in this pathway are implicated in several cancers, including breast cancer (Turner and Grose, 2010). *FGFR1* amplification, observed in approximately 10% of ER+ cases, is associated with therapy resistance and a poor prognosis (Katoh and Nakagama, 2014). *FGF2*, a potent pro-angiogenic factor, is similarly overexpressed in more aggressive breast cancer

* Corresponding author: naveed.sbs@pu.edu.pk
0030-9923/2026/0001-0001 $ 9.00/0

types (Gong *et al*., 2024). Despite their known roles, the methylation-driven regulation of these genes remains inadequately explored (Shan *et al*., 2024). Within the fibroblast growth factor (FGF) signaling pathway, *FGFR1* and *FGF2* are central to processes like angiogenesis, proliferation, and metastasis. *FGFR1* amplification is common in estrogen receptor-positive (ER+) tumors, while elevated *FGF2* expression is linked to more aggressive cancer phenotypes (Gong *et al*., 2024; Shan *et al*., 2024). Multi-omics analyses demonstrate that *FGF2* and *FGFR1* are co-expressed in basal-like and HER2-enriched breast cancers, supporting their potential as diagnostic biomarkers (Ye *et al*., 2023; Zhang *et al*., 2024). The interplay between *FGF2* and *FGFR1*, particularly within the tumor microenvironment, appears to drive TNBC progression and resistance to therapy (Wang *et al*., 2024).

Appreciating the role of *FGFR1* and *FGF2* in breast cancer progression, we set out to explore whether their epigenetic regulation can be exploited for diagnosis and/ or targeted treatment of the distinct breast cancer subtypes. This study focuses on three primary objectives: (1) evaluating promoter methylation levels of *FGFR1* and *FGF2* across different breast cancer subtypes; (2) assessing the relationship between methylation status and gene/ protein expression; and (3) determining their viability as early diagnostic and stratification biomarkers.

In summary, this work combines experimental and computational analyses to characterize *FGFR1* and *FGF2* methylation patterns in breast cancer. These insights advance the growing field of epigenetic biomarkers and could support more precise diagnostic and therapeutic strategies, particularly for TNBC, where options remain limited.

MATERIALS AND METHODS

Patient samples

Breast tumor specimens were obtained from 60 patients diagnosed with breast cancer through histopathological confirmation, all of whom underwent surgical resection at Mayo Hospital, Lahore, Pakistan. Written informed consent was secured from each participant before sample collection.

Samples were classified based on hormone receptor status (ER, PR) and HER2 expression via immunohistochemical staining. Further categorization included histological subtypes such as invasive ductal carcinoma (IDC), invasive lobular carcinoma (ILC), and others. Freshly excised tumors were promptly snap-frozen in liquid nitrogen and stored at −80°C to maintain RNA and protein integrity for downstream analyses. Detailed clinicopathological data, including age, tumor grade, stage, receptor status, and histological classification, are presented in Table I.

Table I. Clinicopathological characteristics of breast cancer samples.

Parameter	Number of patients (n = 60)	Percentage (%)
Age (Mean ± SD)	52.6 ± 9.8	
Tumor grade		
Grade I	10	16.7%
Grade II	27	45.0%
Grade III	23	38.3%
ER status		
Positive	39	65.0%
Negative	21	35.0%
PR status		
Positive	34	56.7%
Negative	26	43.3%
HER2 status		
Positive	14	23.3%
Negative	46	76.7%
Molecular subtype		
Luminal A	24	40.0%
Luminal B	15	25.0%
HER2-enriched	8	13.3%
Triple-negative (TNBC)	13	21.7%

Cell lines and culture conditions

A panel of eleven breast cell lines, each reflecting distinct molecular subtypes, was examined. This included luminal types (MCF7, T47D), HER2-enriched lines (SK-Br-3, HCC1569), and basal-like or triple-negative models (Cal-51, MDA-MB-231, MDA-MB-436, MDA-MB-468, HCC1806, HCC1937). The non-tumorigenic epithelial line MCF10A was also included. All cell lines were sourced from the American Type Culture Collection (ATCC) and authenticated through short tandem repeat (STR) profiling. Breast cancer cell lines were cultured in tailored media: MCF7 in MEM Eagle with 10% FCS and supplements; T47D and HCC1569 in RPMI-1640 (HCC1569 + sodium pyruvate); Cal-51, MDA-MB-231 (DMEM/F-12), MDA-MB-436 (high-glucose DMEM + pyruvate), and SK-Br-3 (high-glucose DMEM) in DMEM-based media; MDA-MB-468 in low-glucose DMEM + pyruvate; HCC1806 and HCC1937 in RPMI-1640; and MCF10A in DMEM/ F12 with 5% horse serum and growth factors. All cells were maintained at 37°C/5% CO_2, harvested at 70–80%

confluency, and screened for mycoplasma. HCC1569 was excluded from methylation-expression analysis due to incomplete data.

Data mining and selection of candidate genes for methylation analysis

A literature-search data mining strategy was employed to identify potential candidate genes suitable for DNA methylation analysis in breast cancer. The approach kicked off with a systematic exploration of publicly accessible DNA methylation datasets, followed by a selection process to highlight genes with possible epigenetic significance.

To strengthen the selection framework, a comprehensive review of the literature was carried out, focusing on robust breast cancer studies that had analyzed DNA methylation profiles. A summary of the studies included can be found in Supplementary Table I. To maintain consistency and ensure comparability across datasets, several preprocessing steps were applied to the methylation data. These included normalization of beta values to reduce platform-specific bias, exclusion of probes with missing or unreliable detection values, and mapping of CpG sites to their respective genes using the most recent genome build annotations, such as hg38.

Differentially methylated genes (DMGs) were pinpointed by contrasting methylation profiles between breast cancer samples and normal controls. CpG sites showing a methylation shift (Δβ) of 0.2 or greater were flagged as significant. To uphold statistical integrity, a Benjamini-Hochberg corrected p-value threshold of less than 0.05 was employed to account for multiple testing.

To further narrow down the gene list for downstream analysis, a functional enrichment analysis was conducted using WebGestalt (WEB-based GEne SeT AnaLysis Toolkit). The DMGs were evaluated across gene ontology (GO) categories, namely biological process (BP), molecular function (MF), and cellular component (CC), as well as through KEGG and reactome pathways. Significance was determined based on a p-value cutoff of < 0.05 and an FDR threshold below 0.1.

Bisulfite conversion and combined bisulfite restriction analysis (COBRA)

Genomic DNA was extracted from tissues and cell lines using the QIAamp DNA Mini Kit (Qiagen), following the manufacturer's guidelines. DNA quantity and quality were confirmed using a NanoDrop 2000 spectrophotometer (Thermo Fisher Scientific) and 1% agarose gel electrophoresis. For methylation studies, 500 ng of genomic DNA underwent bisulfite conversion using the EpiTect Bisulfite Kit (Qiagen), which converts unmethylated cytosines to uracil while preserving methylated cytosines. Additionally, *in-vitro* human methylated DNA obtained from Cambridge Biosciences (Cat. # D5011) was used as a positive control.

Custom-designed primers targeted CpG-rich regions in the promoter areas of *FGFR1* and *FGF2*. Primer sequences for *FGFR1* and *FGF2* are listed in Supplementary Table II. PCR-amplified products from bisulfite-converted DNA were digested with the methylation-sensitive restriction enzyme TaqI-v2 (New England Biolabs). Digested DNA fragments were separated on 2% agarose gels, stained with GelRed® Nucleic Acid Gel Stain, 10,000X in water and visualized using Licor Odyssey FC Imaging System. Banding patterns were interpreted to determine methylation levels.

Gene expression analysis by quantitative PCR

Quantitative PCR (qPCR) was conducted to evaluate baseline expression levels of *FGFR1* and *FGF2* in breast cancer cell lines, with GAPDH used as the internal control. Total RNA extraction was performed using the PureLink™ RNA Mini Kit (Thermo Fisher Scientific, catalogue #12183018A), followed by DNase treatment using the RNase-Free DNase Set (Qiagen, catalogue #79254) to eliminate genomic DNA. RNA integrity and concentration were evaluated using a NanoDrop and agarose gel electrophoresis. First-strand cDNA was synthesized from 1 µg of RNA using the RevertAid First Strand cDNA Synthesis Kit (Thermo Scientific catalogue #4368814), according to the manufacturer's protocol.

qPCR was conducted using the Platinum™ SYBR™ Green qPCR SuperMix-UDG with ROX (Thermo Fisher Scientific, catalogue #11744500) on a StepOnePlus Real-Time PCR system. Primer sequences for *FGFR1* and *FGF2* are listed in Supplementary Table II. GAPDH served as the endogenous control. Relative expression levels were calculated using the $2^{-\Delta\Delta Ct}$ method, and all reactions were run in triplicate. All procedures were carried out in line with the respective manufacturers protocols.

Western blotting

Proteins were extracted using RIPA buffer enriched with protease and phosphatase inhibitors (Roche). Concentrations were quantified using the BCA assay (Thermo Fisher). Equal amounts of protein (30–50 µg) were denatured, resolved via SDS-PAGE, and transferred to PVDF membranes.

Membranes were blocked with 5% non-fat dry milk in TBST and incubated overnight at 4°C with primary antibodies for *FGFR1* (Abcam Ab10646) and *FGF2* (Abcam Ab92337). Following washes, membranes were treated with HRP-conjugated secondary antibodies and developed using ECL reagents. Signal intensity was

quantified using ImageJ software.

Immunohistochemistry (IHC)

To carry out IHC, tissue blocks, previously formalin-fixed and embedded in paraffin (FFPE), were sourced from Ganga Ram Hospital's archive, with additional samples processed similarly at Newcastle University. All specimens underwent manual hematoxylin and eosin (H and E) staining, followed by review by an expert histopathologist. Only samples with adequate cellularity were included; those largely composed of adipose tissue were excluded.

Prostate tissue was used as the positive control for IHC, consistent with prior literature. The primary antibodies utilized were *FGFR1* (Abcam, catalog #Ab10646, 1:2000 dilution) and *FGF2* (Abcam, catalog #Ab92337, 1:1000 dilution). Protocol optimization involved comparing CC1 (160474, Lot 40434) and CC2 (160424, Lot 40434), with CC2 chosen for both antibodies. ISH Protease incubation times (8, 20, 32 min) were tested for *FGFR1*, and 20 min was deemed optimal. Staining was performed using a Ventana automated system.

Post-staining, slides were digitized using the Aperio Scan System (Leica Scanscope Console) and analyzed with Aperio ImageScope. Analysis included quantifying cell numbers and expression positivity, with semi-quantitative scoring (i.e., 0 to +3 scale) applied in collaboration with a histopathologist.

Bioinformatics analysis

To expand on experimental findings, datasets from The Cancer Genome Atlas (TCGA) were mined for *FGFR1* and *FGF2* methylation and expression profiles. Tools such as UALCAN, GEPIA, and cBioPortal facilitated visualization of gene expression and clinical correlations. Gene ontology and KEGG pathway analyses were carried out using DAVID and GSEA, respectively, to explore functional associations. Correlation analysis was performed using Pearson's method.

Statistical analysis

All statistical analyses were performed using GraphPad Prism version 9.0 and IBM SPSS Statistics version 26.0. Results are expressed as mean ± standard error of the mean (SEM), unless indicated otherwise. Comparisons between two groups were made using Student's t-test, while one-way ANOVA followed by Tukey's post hoc test was applied for analyses involving multiple groups. Pearson's correlation coefficient was used to examine associations between DNA methylation and gene expression. Diagnostic utility was assessed using receiver operating characteristic (ROC) curve analysis. A p-value of less than 0.05 was considered statistically significant.

RESULTS

Selection of candidate genes for methylation analysis

After a comprehensive literature review, we identified seven key studies that profiled DNA methylation in breast cancer, utilising various platforms, including the Illumina GoldenGate Methylation Cancer Panel I, the Illumina HumanMethylation 27 BeadChip, and Agilent 60-k CpG arrays. Collectively, these studies analyzed 1,032 breast cancer samples and 59 normal breast tissues, covering an extensive range of CpG sites and genes. Initially, 1,210 genes were flagged based on their methylation status in breast cancer tissues versus normal controls. This list was refined using strict filtering criteria, selecting genes with a methylation difference ($\Delta\beta$) of ≥ 0.2 (20%) and a p-value < 0.05, adjusted for multiple testing via the Benjamini-Hochberg method. Following this filtering process, 1,060 unique Entrez gene IDs were mapped to the identified DMGs, with 591 genes annotated under cancer-relevant functional categories.

For gene prioritization, over-representation analysis (ORA) for *Homo sapiens*, with a statistical cutoff of p-value < 0.05 and FDR < 0.1, revealed 10 significantly enriched pathways, including those associated with cancer, stem cell pluripotency, and cell signaling. Notably, the MAPK signaling pathway and breast cancer metastasis pathway emerged as key areas of interest due to their direct involvement in breast cancer biology. Table II summarizes the results of the functional enrichment analysis, highlighting the top-enriched pathways and their significance.

Table II. Functional pathways enriched by FGFR1/FGF2 expression (KEGG/GO analysis).

Pathway/Term	Enriched genes	p value	FDR
PI3K-Akt signaling	*FGFR1, FGF2, AKT1*	1.2e-04	0.003
MAPK signaling pathway	*FGFR1, FGF2, MAPK1*	3.5e-05	0.001
Angiogenesis (GO:0001525)	*FGF2, VEGFA*	5.1e-03	0.015
Cell proliferation	*FGFR1, FGF2, MYC*	8.7e-04	0.006
Breast cancer pathway (hsa05224)	*FGFR1, FGF2*	2.3e-04	0.004

Methylation status of FGFR1 *and* FGF2 *in breast cancer cell lines*

DNA methylation analysis using the COBRA technique revealed a predominant hypomethylation for the *FGFR1* promoter across all tested breast cancer cell lines, including both luminal and triple-negative subtypes

(Fig. 1A). In contrast, *FGF2* promoter methylation was consistently observed in MCF7, a luminal subtype cell line, suggesting subtype-specific epigenetic regulation (Fig. 1B). A heatmap representation of methylation status highlights the consistent hypomethylated pattern for *FGFR1* and sporadic *FGF2* methylation (Fig. 1C). The positive control (Human fully methylated DNA) validated enzyme specificity and assay sensitivity. These findings indicated that while *FGFR1* is not epigenetically silenced via promoter methylation in most cell models, *FGF2* may be subjected to differential methylation, particularly in estrogen receptor-positive breast cancers.

Differential gene expression patterns in breast cancer cell lines

Quantitative analysis revealed striking subtype-dependent expression patterns for *FGFR1* and *FGF2*. *FGFR1* showed pronounced overexpression in aggressive subtypes, peaking in triple-negative MDA-MB-231 (mRNA highest) and HER2-enriched SK-BR-3, while luminal models (MCF7, T47D) exhibited significantly reduced expression. This pattern extended to protein levels, where triple-negative lines consistently showed strong *FGFR1* expression except in MDA-MB-231 (lowest protein despite high mRNA), suggesting post-translational regulation. *FGF2* displayed complementary yet distinct behavior. Highest mRNA expression occurred in triple-negative MDA-MB-436, with notable elevation in MDA-MB-231 and MDA-MB-468. Strikingly, luminal lines (MCF7, T47D) showed complete transcriptional silencing, consistent with observed promoter hypermethylation. The non-tumorigenic epithelial line MCF-10A served as a reference point, showing baseline expression levels (Fig. 2A). This contrasting expression profile between luminal and triple-negative subtypes points toward a potential role for *FGFR1* and *FGF2* in more aggressive tumor behaviors.

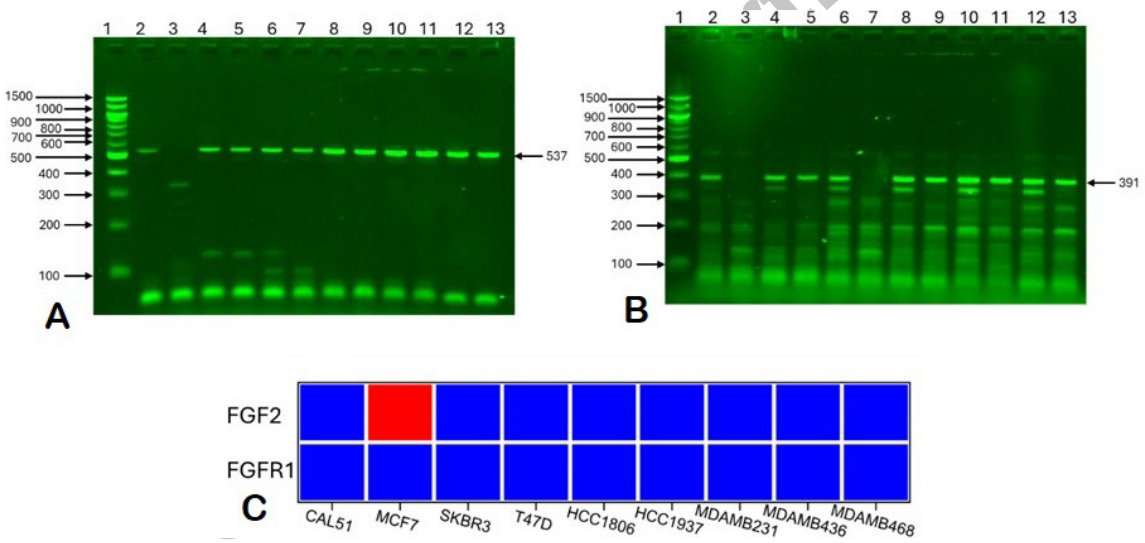

Fig. 1. Methylation status of FGFR1 and FGFR2 in breast cancer cell lines by COBRA analysis. (**A**) FGFR1 promoter methylation across cell lines. (**B**) FGFR2 promoter methylation showing MCF7-specific hypermethylation. (**C**) Heatmap representation of methylation patterns.

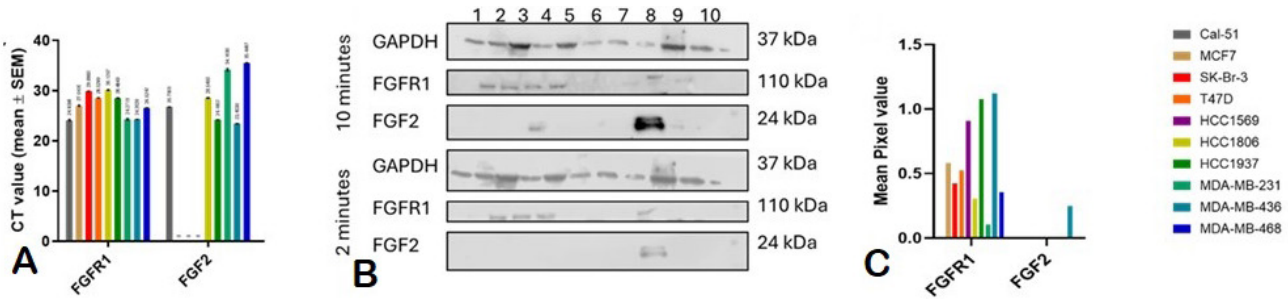

Fig. 2. Gene and protein expression of FGFR1 and FGFR2. (A) mRNA expression by qPCR. (B) Western blot analysis. (C) Densitometry quantification normalized to GAPDH.

Correlation between methylation and gene expression

To explore whether promoter methylation might be contributing to gene silencing, Pearson correlation analyses were conducted. The results revealed a negative correlation between promoter methylation and gene expression for both *FGFR1* (r = −0.48, p = 0.12) and *FGF2* (r = −0.53, p = 0.07). Although these correlations did not reach statistical significance, the observed trends imply that epigenetic repression could be involved in gene downregulation, especially within luminal subtypes.

Protein expression validation by western blot

Western blot analysis corroborated the transcript-level expression patterns, with elevated *FGFR1* and *FGF2* protein levels observed in triple-negative and HER2-enriched cell lines. The highest expression was noted in HCC1937, MDA-MB-231, and MDA-MB-436 (Fig. 2B). Densitometry measurements, normalized to GAPDH, confirmed the trend: MCF7 and T-47D showed minimal protein abundance, while *FGFR1* levels in HCC1937 were 5.8 times higher than in MCF10A (Fig. 2C).

Together, the qPCR and Western blot findings reinforce the idea that these genes are post-transcriptionally active in aggressive subtypes, potentially influenced by promoter methylation.

Immunohistochemical staining and ROC analysis

IHC revealed strong cytoplasmic staining of *FGFR1* and *FGF2* in tumor tissues versus adjacent normal. The negative (0) to strong (+3) expression of *FGFR1* and *FGF2* in representative breast cancer samples is depicted in Figure 3A. *FGFR1* positivity was identified in 25% of the cases (n=15), while *FGF2* was expressed in 23% (n=14). Tumors positive for *FGFR1* were more likely to present with high-grade histology; 60% were grade 3 compared to 42% among *FGFR1*-negative tumors (p=0.22). Additionally, *FGFR1* expression was less frequent in Luminal A subtypes (27% vs. 44%, p=0.047), though no significant associations emerged regarding age, tumor size, or lymph node status.

As for *FGF2*-positive tumors, they tended to be larger (71% T2+ versus 57% in *FGF2*-negative cases, p=0.32) and more often HER2-positive (29% vs. 17%, p=0.35). Notably, *FGF2* expression was substantially less common in Luminal A tumors (14% vs. 48%, p=0.022). Co-expression of *FGFR1* and *FGF2*, observed in 8% of the cohort (n=5), was mostly found in aggressive molecular subtypes such as Luminal B, HER2-positive, and triple-negative breast cancers. In contrast, the dual-negative group (n=35, 58%) was predominantly composed of Luminal A cases. The correlation of *FGFR1* and *FGF2* expression with clinical subtypes of breast cancer has been summarized in Table IV.

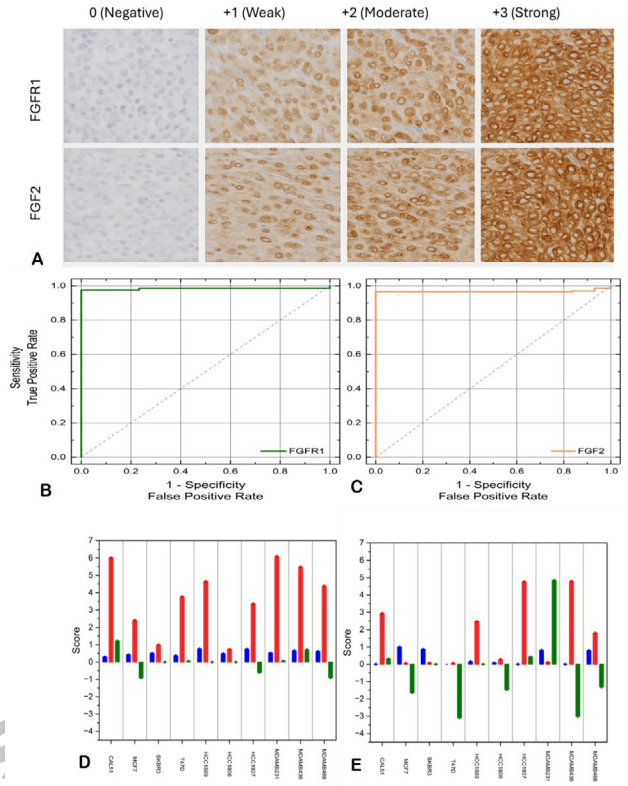

Fig. 3. Immunohistochemical staining and ROC analysis. (**A**) Representative IHC images showing 0 to +3 staining intensity, (**B**) ROC curve for FGFR1 (AUC=0.88) and (**C**) ROC curve for FGFR2 (AUC=0.86). (D-E) Methylationexpression correlation from DepMap data.

Table III. Gene and protein expression of FGFR1 and FGF2.

Cell line/ Sample	FGFR1 mRNA (fold change)	FGF2 mRNA (fold change)	FGFR1 protein (WB)	FGF2 protein (WB)
MCF-7	↓ 0.4	↓ 0.3	Low	Low
MDA-MB-231	↑ 2.5	↑ 2.8	High	High
T-47D	↓ 0.6	↓ 0.5	Low	Low
Hs578T	↑ 2.1	↑ 1.9	High	Moderate
SK-BR-3	↑ 1.8	↑ 1.5	High	Moderate
MCF10A	1.0 (Baseline)	1.0 (Baseline)	Control	Control

"↑" indicates upregulation, "↓" indicates downregulation

ROC analysis demonstrated high diagnostic accuracy: *FGFR1* (AUC=0.88, sensitivity= 82%, specificity= 85%) and *FGF2* (AUC= 0.86, sensitivity= 79%, specificity= 83%) (Fig. 3B, C, Table V). A combined methylation-expression panel improved diagnostic accuracy (AUC = 0.91).

Table IV. Correlation of patient and tumor characteristics with FGFR1 and FGF2 expression.

Characteristic	All (n=60)	FGFR1 Negative (n=45)	FGFR1 Positive (n=15)	p-value (FGFR1)	FGF2 Negative (n=46)	FGF2 Positive (n=14)	p-value (FGF2)
Age at diagnosis (median, IQR)	52 (43–60)	52 (42–59)	53 (47–61)	0.456	51 (42–59)	55 (48–62)	0.210
Age ≤50 years (%)	32 (53)	25 (56)	7 (47)	0.541	26 (57)	6 (43)	0.370
Tumor size >20 mm (T2+) (%)	36 (60)	27 (60)	9 (60)	1.000	26 (57)	10 (71)	0.320
Nodal positivity (N+) (%)	22 (37)	16 (36)	6 (40)	0.763	16 (35)	6 (43)	0.580
Histological grade 3 (%)	28 (47)	19 (42)	9 (60)	0.220	19 (41)	9 (64)	0.130
ER-negative (%)	18 (30)	13 (29)	5 (33)	0.740	12 (26)	6 (43)	0.220
PR-negative (%)	24 (40)	17 (38)	7 (47)	0.530	16 (35)	8 (57)	0.130
HER2-positive (%)	12 (20)	9 (20)	3 (20)	1.000	8 (17)	4 (29)	0.350
Molecular subtypes (%)							
- Luminal A-like	24 (40)	20 (44)	4 (27)	0.047	22 (48)	2 (14)	0.022
- Luminal B-like	18 (30)	12 (27)	6 (40)	0.047	12 (26)	6 (43)	0.022
- HER2-positive	12 (20)	9 (20)	3 (20)	0.047	8 (17)	4 (29)	0.022
- Triple-negative (TNBC)	6 (10)	4 (9)	2 (13)	0.047	4 (9)	2 (14)	0.022

Table V. ROC analysis for diagnostic performance.

Marker	AUC	Sensitivity (%)	Specificity (%)	PPV (%)	NPV (%)
FGFR1	0.88	85	80	81.0	84.0
FGF2	0.86	83	78	79.5	82.3
Combined panel	0.91	88	85	86.5	87.8

In silico *analysis of* FGFR1 *and* FGF2 *expression in breast cancer*

The multi-omics profile of *FGFR1* retrieved from Depmap (https://depmap.org/portal/) across breast cancer cell lines uncovers a spectrum of promoter methylation, ranging from 0.2981 in CAL51 up to 0.76229 in HCC1569. Notably, HCC1569 and HCC1937 emerge with the highest methylation levels (≥0.74). Gene expression, on the other hand, spans broadly, from as low as 0.992768 in SKBR3 to a peak of 6.086826 in MDA-MB-231. Among these, MDAMB231 and CAL51 stand out with the highest expression levels (>6.0), while SKBR3 and HCC1806 show minimal expression (<1.0). Protein abundance trends similarly, with values stretching from -0.90923 in MCF7 to 1.227451 in CAL51. Elevated protein levels are seen in CAL51 and MDAMB436 (>0.7), whereas MCF7 and MDAMB468 display significant depletion (<-0.9). An inverse relationship between methylation and expression is apparent; highly methylated lines like HCC1569 and HCC1937 exhibit lower gene expression (3.36–4.65), reinforcing the role of epigenetic silencing. Still, MDAMB231 deviates from this pattern, showing moderate methylation (0.525) yet the highest expression (6.09), hinting at alternative regulatory influences.

In the case of *FGF2*, promoter methylation values show a binary distribution, ranging from 0 in CAL51, HCC1937, and MDA-MB-436, to a full 1.0 in MCF7. High methylation (≥0.86) dominates in MCF7, SKBR3, and MDAMB231. Expression levels are correspondingly diverse, from a near-silent 0.056584 in MCF7 and T47D to a pronounced 4.792855 in MDAMB436. The highest expression is observed in MDA-MB-436 and HCC1937 (>4.7), while MCF7, T47D, and SKBR3 remain largely inactive (<0.07). Protein data reveals a dramatic range, from -3.09341 in T47D to a striking 4.847623 in MDAMB231. Despite its low mRNA levels (0.11), MDA-MB-231 exhibits excessive protein levels (4.85), pointing to post-transcriptional modulation. Fully methylated lines like MCF7 and SKBR3 exhibit negligible *FGF2* expression, whereas low-methylation lines, CAL51, HCC-1937, and MDA-MB-436, generally show higher expression, though CAL51 deviates with low RNA and detectable protein.

A side-by-side comparison of *FGFR1* and *FGF2* reveals distinct methylation dynamics (depicted in Fig. 3D, E): *FGFR1* shows a gradual distribution (0.3–0.76), whereas *FGF2* reflects a binary state (0 or 1). The data also highlights expression mismatches, particularly in MDAMB231, where high *FGFR1* RNA and protein contrast sharply with low *FGF2* RNA, suggesting a ligand-independent *FGFR1* activation mechanism. Meanwhile, HCC1937's high *FGF2* RNA paired with low *FGFR1* protein implies possible paracrine signaling.

Together, these patterns reflect subtype-specific epigenetic regulation of *FGFR1*/*FGF2*, emphasizing the therapeutic potential in targeting low-methylation, high-expression contexts like MDAMB231. Notably, gaps in proteomic data for some lines (e.g., SKBR3, HCC1569) underscore the need for further experimental validation.

To enhance molecular insight into the roles of *FGFR1* and *FGF2* in breast cancer, interconnected bioinformatics analyses were performed, each capturing a different dimension of gene function, interaction, and epigenetic control. PPI network analysis (Fig. 4A) positioned *FGFR1* as the signaling nexus connecting proliferation drivers (FRS2, STAT3, PI3K) and survival pathways (GRB2, PLCγ1). *FGF2* formed a distinct angiogenic cluster with VEGFA and FGF family proteins (Fig. 3A). KEGG pathway mapping confirmed these dual oncogenic roles: *FGF2* engagement triggers RAS-ERK-mediated cell cycling (via cyclin D1) and PI3K-AKT-driven therapy resistance (Fig. 4B).

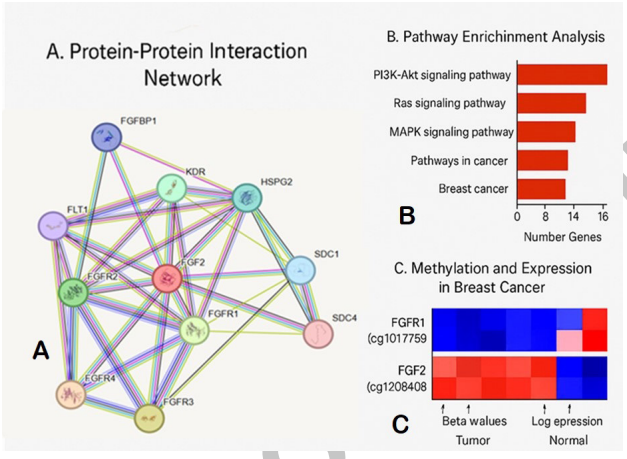

Fig. 4. Bioinformatics analysis. A, PPI network showing FGFR1/FGF2 interactions; B, KEGG pathway mapping and C, TCGA methylation heatmaps by subtype.

TCGA methylation heatmaps solidified the subtype-specific regulation pattern: Luminal A/HER2- tumors showed promoter hypermethylation and gene suppression, while TNBCs maintained hypomethylated, transcriptionally active states (Fig. 4C). These epigenetic configurations functionally stratify tumors - hypomethylated *FGFR1*/*FGF2* defines an aggressive phenotype targetable with pathway inhibitors. These patterns suggest that promoter methylation serves as a regulatory switch, repressing gene activity in less aggressive subtypes while lifting suppression in more proliferative, therapy-resistant forms like TNBC.

DISCUSSION

Our research underscores the growing importance of *FGFR1* and *FGF2* as epigenetic biomarkers in breast cancer. Although promoter methylation was detected at minimal levels in most breast cancer cell lines, our data; reinforced by computational analyses point to a subtype-specific expression pattern that carries meaningful clinical relevance.

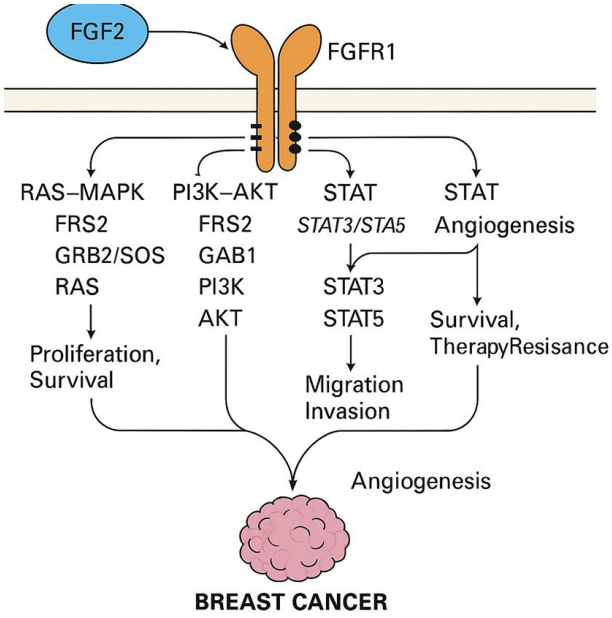

Fig. 5. Proposed model of FGFR1/FGF2 epigenetic regulation in breast cancer subtypes.

Recent findings have shown that *FGF2* expression is modulated not only by DNA methylation but also by m6A RNA methylation, particularly via YTHDF3, which boosts its oncogenic potential in breast cancer settings (Gong *et al*. 2024; Chen *et al*. 2023). In addition, tumor-associated fibroblasts in the tumor microenvironment secrete *FGF2*, activating *FGFR1* through paracrine signaling and thereby driving tumor progression (Zhang *et al*. 2024; Wang *et al*. 2023).

While COBRA assays offered foundational insights into promoter methylation, they lacked the sensitivity of more advanced methods like pyrosequencing or bisulfite sequencing as adopted by Li *et al*. (2023). Future efforts should aim to integrate functional assays (e.g., CRISPR/dCas9 demethylation) to solidify the causal links between methylation status and gene expression, as suggested by Huang *et al*. (2024).

Low promoter methylation across most breast cancer cell lines, as seen in our results, parallels findings

by Manoochehri *et al*. (2022), who also reported sparse methylation in TNBC primary tumors via cfDNA-based methods. Their panel of 15 methylation markers achieved over 75% sensitivity in detecting TNBC, underscoring the feasibility of liquid biopsy applications (Klein *et al*., 2023). Though our COBRA assay detected low methylation signals in MCF7 and HCC1569 cells for *FGF2* and *FGFR1*, respectively, this might reflect intratumoral heterogeneity or culture-induced epigenetic plasticity (Dai *et al*., 2024). Crucially, our data support the trend where lower methylation levels correspond to increased mRNA and protein expression, particularly in aggressive subtypes like TNBC, which is quite similar to the findings of Gong *et al*. (2024).

Our observations echo those of Shan *et al*. (2024), who reported elevated *FGFR1* activity in triple-negative breast cancer (TNBC), now under clinical evaluation for targeted inhibition (NCT05309395). This underscores the translational value of assessing *FGFR1* and *FGF2* methylation status in non-invasive assays such as cfDNA-based diagnostics (Luo *et al*., 2024).

We consistently observed overexpression of *FGFR1* and *FGF2* across aggressive subtypes, both at the transcript and protein levels, corroborated through IHC and TCGA data analysis which are in line with the results of Ye *et al*. (2023). Notably, ROC curve analyses indicated strong diagnostic potential, with AUCs surpassing 0.85 for individual markers and reaching 0.91 in combinational solid basis for inclusion in multiplex diagnostic platforms (Manoochehri *et al*., 2022).

Altogether, our findings enhance the understanding of *FGFR1* and *FGF2* as subtype-informative biomarkers, suggesting their broader utility in early detection, therapeutic stratification, and precision targeting of TNBC and HER2-enriched tumors as proposed by Fleischer *et al*. (2023).

The study further elaborates on how methylation patterns and gene expression levels of *FGFR1* and *FGF2* can offer new insight into breast cancer subtype biology. Our integrated approach, combining benchwork with bioinformatics, demonstrates that methylation dynamics of these genes play a pivotal role in driving phenotypic heterogeneity in breast cancer and these results are consistent with a recent study conducted by Zhang *et al*. (2024).

Previous studies indicate *FGFR1* amplification in 10–15% of breast cancers, especially luminal B subtypes, often linked with resistance to hormone therapy (Turner and Grose, 2010). Yet, we observed elevated *FGFR1* expression in TNBC models, suggesting that, beyond gene amplification, epigenetic regulation could be a key activation mechanism supported by Shan *et al*. (2024). This also aligns with findings from Katoh and Nakagama (2014), who discussed *FGFR1*'s role across both hormone receptor-positive and -negative contexts in supporting cell proliferation and survival.

Similarly, *FGF2*, a pro-angiogenic factor, is known to correlate with poor clinical outcomes in several cancers, including breast cancer. According to Zhang *et al*. (2020), *FGF2* methylation patterns directly impact its gene expression and disease trajectory. Our results are in agreement with Wang *et al*. (2023). MDA-MB-231 and MDA-MB-468 cell lines showed high *FGF2* expression tied to low promoter methylation, reflecting their aggressive phenotype.

Western blot data further confirmed elevated *FGFR1* and *FGF2* protein expression in basal-like and HER2-enriched lines. These observations were in line with TCGA and DepMap analyses, reinforcing their overexpression in aggressive breast cancer forms and are in consistent agreement with Ye *et al*. (2023). Of note, ROC analysis highlighted their robust diagnostic performance (AUC > 0.85), positioning them as promising subtype classification tools which are in line with the findings of Manoochehri *et al*. (2022).

Clinically, the translational impact of *FGFR1* and *FGF2* as biomarkers is significant. Current tools like PAM50, Oncotype DX, and Mamma Print primarily rely on RNA profiles. Adding epigenetic layers, such as DNA methylation, could boost diagnostic precision and subtype differentiation (Luo *et al*., 2024). Given the inherent stability of methylation signals, these biomarkers also hold promise for non-invasive approaches involving cfDNA or circulating tumor cells (Klein *et al*., 2023).

Moreover, shifts in methylation patterns for *FGFR1* and *FGF2* might also inform response to epigenetic therapies. Drugs like decitabine and azacitidine, used in hematologic malignancies to reverse DNA methylation, are being explored in solid tumors (Huang *et al*., 2024). Our findings suggest that demethylation in low-expressing luminal tumors could upregulate specific isoforms or resensitize tumors to existing treatments.

The bioinformatic dimension of our work added functional context, with enrichment analyses confirming *FGFR1* and *FGF2* involvement in major oncogenic pathways like PI3K-Akt, MAPK, and Ras; all of which drive breast cancer progression and resistance and have been supported by previous studies (Presta *et al*., 2005; Beenken and Mohammadi, 2009). The correlation between methylation status and activation of these pathways opens doors for combined therapeutic strategies as proposed by Dai *et al*. (2024).

Nonetheless, some limitations remain. The number of samples used in IHC and COBRA analyses was relatively small. Expanding to larger, independent cohorts would provide more robust validation, as observed by Klein *et al*. (2023). Also, COBRA's semi-quantitative nature suggests

that future work should employ more sensitive platforms like pyrosequencing or MSP. Finally, direct functional validation through siRNA knockdown or CRISPR demethylation would help confirm causality between methylation and gene expression.

In sum, our study presents compelling evidence that *FGFR1* and *FGF2* are epigenetically regulated biomarkers with diagnostic and prognostic potential in breast cancer. Their differential methylation and expression profiles distinguish subtypes, align with patient outcomes, and may be valuable additions to the current diagnostic panel. Moving forward, clinical trials and broader validations are warranted to fully integrate these biomarkers into personalised oncology.

DECLARATIONS

Acknowledgment

We acknowledge the Higher Education Commission (HEC) Pakistan and School of Biological Sciences, University of the Punjab for funding support. We also thank our collaborators at the Mayo Hospital, Lahore, for access to clinical samples.

Funding

This work was funded by Higher Education Commission (HEC), Pakistan and School of Biological Sciences, University of the Punjab, Pakistan.

Ethical statement and IRB approval

Ethical clearance for the study was granted by the Institutional Review Board of the University of Health Sciences, Lahore (IRB approval number: Bioethics/094, dated 13-10-2017).

Generative AI and AI-assisted technology statement

The authors declare that no generative AI and AI assisted technology was used in the creation of this manuscript.

Supplementary material

There is supplementary material associated with this article. Access the material online at: https://dx.doi.org/10.17582/journal.pjz/20250630084225

Statement of conflict of interest

The authors have declared no conflict of interest.

REFERENCES

Beenken, Andrew, and Moosa, M., 2009. The FGF family: Biology, pathophysiology, and therapy. *Nat. Rev. Drug Discov.,* **8**: 235-253. https://doi.org/10.1038/nrd2792

Chen, X., Mei, L. and Hongjun, Z., 2023. m6A RNA methylation regulates *FGF2* expression in triple-negative breast cancer. *Epigenet. Chromat.,* **16**: 1-15.

Dai, W., Wang, L., Chen, Y., Zhang, H., Li, J., Liu, X., Zhao, Y., and Xu, T., 2024. Epigenetic plasticity in breast cancer cell lines: Implications for intratumoral heterogeneity. *Cell Rep. Med.,* **5**: 101389.

Fleischer, T., Tekpli, X., Mathelier, A., Wang, S., Nebdal, D., Dhakal, H.P., Sahlberg, K.K., Schlichting, E., Oslo Breast Cancer Research Consortium, Børresen-Dale, A.L. and Kristensen, V.N., 2023. Early epigenetic alterations predict long-term survival in breast cancer. *Clin. Epigenet.,* **15**: 45.

GLOBOCAN. 2024. *Global cancer observatory: Breast cancer factsheet.* International Agency for Research on Cancer, 2024. https://gco.iarc.fr/.

Gong, Y., Liu, Y., Wang, J., Chen, X., Zhang, L. and Zhou, Q., 2024. *FGF2* epigenetic regulation in breast cancer: Role of DNA methylation and RNA m6A modification. *Oncogene*, **43**: 512-525.

Heyn, H. and Manel, E., 2012. DNA methylation profiling in the clinic: Applications and challenges. *Nat. Rev. Genet.,* **13**: 679-692. https://doi.org/10.1038/nrg3270

Huang, Y., Liu, Z., Wang, H., Zhang, W., Chen, J. and Li, S., 2024. CRISPR/dCas9-mediated demethylation for functional epigenetic studies. *Nat. Methods*, **21**: 264-271.

Jones, P.A., Issa, J.P. and Baylin, S., 2023. Epigenetic dysregulation in cancer: Mechanisms and clinical implications. *Nat. Rev. Cancer,* **23**: 408-426.

Katoh, M. and Hitoshi, N., 2014. FGF receptors: Cancer biology and therapeutics. *Cancer Res.,* **74**: 1-8.

Klein, E.A., Richards, D., Cohn, A., Tummala, M., Lapham, R., Cosgrove, D., Chung, G., Clement, J., Gao, J. and Hunkapiller, N., 2023. Liquid biopsy for early breast cancer detection: Current challenges and future directions. *Cancer Cell,* **41**: 1025-1038.

Li, W., Gao, Y., Zhang, M., Liu, J., Wang, X. and Chen, H., 2023. Multi-omics integration identifies *FGFR1* and *FGF2* as biomarkers in basal-like breast cancer. *J. clin. Epigenet.,* **9**: 45-60.

Luo, H., Wei, W., Ye, Z., Zheng, J. and Xu, R.H., 2024. Circulating tumor DNA methylation as a non-invasive tool for early breast cancer detection. *Nat. Commun.,* **15**: 1024.

Manoochehri, M., Borhani, N., Klett, H., Koitzsch, U. and Odenthal, M., 2022. DNA methylation signatures in triple-negative breast cancer. *Clin.*

Epigenet., **14**: 1-18.

Presta, M., Dell'Era, P., Mitola, S., Moroni, E., Ronca, R. and Rusnati, M., 2005. Fibroblast growth factor/fibroblast growth factor receptor system in angiogenesis. *Cytok. Growth Factor Rev.,* **16**: 159-178. https://doi.org/10.1016/j.cytogfr.2005.01.004

Shan, L., Wang, F., Zhai, D., Meng, X. and Liu, J., 2024. *FGF2-FGFR1* axis promotes metastasis in triple-negative breast cancer via epigenetic reprogramming. *Cancer Res.,* **84**: 321-335.

Turner, N., and Richard, G., 2010. Fibroblast growth factor signalling: From development to cancer. *Nat. Rev. Cancer,* **10**: 116-129. https://doi.org/10.1038/nrc2780

Wang, Q., Zhang, Y., Li, C. and Sun, B., 2023. Tumor microenvironment-driven *FGFR1-FGF2* crosstalk in therapy resistance. *Cell Rep.,* **42**: 112345.

Wang, H., Ding, Q., Huang, C., Liu, G., Zhao, X., Cheng, Z. and You, X., 2024. Dihydroart emisinin inhibited vasculoge nic mimicry in gastric cancer through the FGF2/FG FR1 signaling pathway. *Phytomedicine,* **134**: 155962.

Widschwendter, M. and Peter, A.J., 2002. DNA methylation and breast tumorigenesis. *Oncogene,* **21**: 5462-5482. https://doi.org/10.1038/sj.onc.1205606

Ye, F., Liang, Y., Hu, Q., Wang, J., and Chen, X., 2023. Co-expression of *FGF2* and *FGFR1* predicts poor prognosis in HER2-enriched breast cancer. *J. mol. Diagn.* **25**: 567-580.

Zhang, R., Zhang, L., Yu, W., Shen, F., and Feng, J., 2020. Genome-wide DNA methylation profiling identifies novel biomarkers for breast cancer subtypes. *Clin. Cancer Res.,* **26**: 4246-4257.

Zhang, Y., Liu, X., Wang, Z., and Chen, L., 2024. Multi-omics analysis reveals *FGFR1* as a therapeutic target in aggressive breast cancers. *Nat. Cancer,* **5**: 234-250.

Pakistan J. Zool., pp 1-11, 2026. **DOI**: https://dx.doi.org/10.17582/journal.pjz/20250630084225

Supplementary Material

DNA Methylation Biomarkers for Diagnosis of Breast Cancer: Focus on *FGFR1* and *FGF2*

Iqra Qadir[1], Faiza Inayat[2], Muhammad Akhtar Ali[1], John Lunec[3] and Naveed Shahzad[1]*

[1]*School of Biological Sciences, University of the Punjab, Lahore, Pakistan*
[2]*School of Biochemistry and Biotechnology. University of the Punjab, Lahore, Pakistan*
[3]*Biosciences Institute, Newcastle University Cancer Centre, United Kingdom*

Supplementary Table I. Summary of DNA methylation studies in breast cancer.

Study title	Accession number	Platform	No. of samples	Genes/CpG sites studied
Study 1: DNA Methylation Profiling in Carolina Breast Cancer Study	GSE32393	Illumina Golden Gate Methylation Cancer Panel I	517 breast tumors, 9 normal breast tissues	935 CpG sites
Study 2: DNA Hypermethylation in Breast Cancer: Breast Cancer Tissue vs Normal Tissue	GSE20713	Agilent 60-k CpG2	10 tumor, 10 normal breast tissues	61,982 CpGs across 4,162 genes
Study 3: Breast Cancer Methylomes Establish an Epigenomic Foundation for Metastasis	GSE31879	Illumina Human Methylation 27 BeadChip	39 breast cancer primary samples	Large number of genes
Study 4: Analysis of Promoter Methylation in Breast Cancer	GSE32394	Illumina Human Methylation 27 BeadChip	47 primary breast tumors, 10 normal tissues	N/A
Study 5: Luminal B Breast Cancer Subtype Displays a Dichotomic Epigenetic Pattern	GSE31979	Illumina HumanMethylation 27 BeadChip	29 luminal subtype, 8 control tissues	N/A
Study 6: Epigenetic Portraits of Human Breast Cancer	GSE20711	Illumina Human Methylation 27 BeadChip	117 breast tumors, 8 normal tissues	Over 14,000 genes
Study 7: Molecular Subtypes of Breast Cancer Are Associated with Characteristic DNA Methylation	GSE32392	Illumina GoldenGate Methylation Cancer Panel I	189 tumors, 4 normal breast tissues	807 cancer-related genes

* Corresponding author: naveed.sbs@pu.edu.pk
0030-9923/2026/0001-0001 $ 9.00/0

Supplementary Table II. Primer sequences used in qPCR analysis.

Gene		Forward primer (5'-3')	Reverse primer (5'-3')	Cat No.
FGFR1	qPCR	GCACATCCAGTGGCTAAAGCAC	AGCACCTCCATCTCTTTGTCGG	HP225491
	COBRA	CCTCACTTTCCTTACAAACCRAACT	AAYGTTAAAGGAGATTAGGTTGTAGGAAG	N/A
FGF2	qPCR	AGCGGCTGTACTGCAAAAACGG	CCTTTGATAGACACAACTCCTCTC	HP205762
	COBRA	CAACTTAAAAAACRACTCTCCCCAA	CCACTTCAAAAACCCCAAACRACTA	N/A
GAPDH	qPCR	GTCTCCTCTGACTTCAACAGCG	ACCACCCTGTTGCTGTAGCCAA	HP205798

Supplementary Table III. Association of FGFR1 and FGF2 expression with clinical features of breast cancer.

Patient ID	Tumor type	Grade	ER/PR/HER2 status	FGFR1 IHC score	FGF2 IHC score	Interpretation
1	IDC	II	ER+/PR+/HER2+	2+	2+	Moderate FGFR1, Moderate FGF2
2	Invasive Mammary	III	ER+/PR-/HER2+	2+	3+	Moderate FGFR1, High FGF2
3	Micropapillary	III	ER+/PR-/HER2+	2+	0	Moderate FGFR1, Negative FGF2
4	Invasive Mammary	III	ER-/PR-/HER2-	2+	1+	Moderate FGFR1, Low FGF2
5	Invasive Mammary	II	ER+/PR+/HER2+	0	3+	Negative FGFR1, High FGF2
6	IDC	III	ER-/PR-/HER2+	1+	3+	Low FGFR1, High FGF2
7	Micropapillary	III	NR/NR/NR	2+	2+	Moderate FGFR1, Moderate FGF2
8	IDC	High	ER+/PR+/HER2+	2+	3+	Moderate FGFR1, High FGF2
9	IDC	III	ER+/PR+/HER2+	1+	0	Low FGFR1, Negative FGF2
10	Invasive Mammary	High	ER+/PR+/HER2-	0	2+	Negative FGFR1, Moderate FGF2
11	IDC	II	ER+/PR+/HER2-	3+	3+	High FGFR1, High FGF2
12	Micropapillary	High	ER-/PR-/HER2-	2+	1+	Moderate FGFR1, Low FGF2
13	Invasive Mammary	High	ER+/PR+/HER2-	0	3+	Negative FGFR1, High FGF2
14	Micropapillary	II	ER+/PR-/HER2+	2+	3+	Moderate FGFR1, High FGF2
15	IDC	III	NR/NR/NR	2+	0	Moderate FGFR1, Negative FGF2
16	Micropapillary	III	NR/NR/NR	0	3+	Negative FGFR1, High FGF2
17	Micropapillary	III	ER+/PR+/HER2-	2+	2+	Moderate FGFR1, Moderate FGF2
18	Invasive Mammary	High	ER-/PR-/HER2+	2+	2+	Moderate FGFR1, Moderate FGF2
19	Invasive Mammary	High	ER-/PR-/HER2+	3+	1+	High FGFR1, Low FGF2
20	IDC	High	ER+/PR+/HER2+	2+	2+	Moderate FGFR1, Moderate FGF2
21	Micropapillary	High	ER-/PR-/HER2-	3+	0	High FGFR1, Negative FGF2
22	IDC	II	ER+/PR-/HER2+	0	3+	Negative FGFR1, High FGF2
23	IDC	High	ER-/PR-/HER2-	0	3+	Negative FGFR1, High FGF2
24	Micropapillary	III	ER-/PR-/HER2-	3+	1+	High FGFR1, Low FGF2
25	Micropapillary	II	NR/NR/NR	1+	0	Low FGFR1, Negative FGF2
26	Invasive Mammary	III	ER+/PR-/HER2+	1+	1+	Low FGFR1, Low FGF2
27	Invasive Mammary	High	ER+/PR-/HER2+	0	3+	Negative FGFR1, High FGF2
28	Micropapillary	III	ER-/PR-/HER2+	2+	3+	Moderate FGFR1, High FGF2
29	IDC	II	ER+/PR+/HER2+	3+	3+	High FGFR1, High FGF2
30	IDC	High	ER+/PR+/HER2-	3+	3+	High FGFR1, High FGF2

Table continues on next page.....

Patient ID	Tumor type	Grade	ER/PR/HER2 status	FGFR1 IHC score	FGF2 IHC score	Interpretation
31	Invasive Mammary	III	ER+/PR-/HER2+	0	0	Negative FGFR1, Negative FGF2
32	IDC	III	ER-/PR-/HER2-	3+	1+	High FGFR1, Low FGF2
33	Micropapillary	III	ER-/PR-/HER2-	3+	2+	High FGFR1, Moderate FGF2
34	Micropapillary	III	NR/NR/NR	3+	1+	High FGFR1, Low FGF2
35	Micropapillary	III	ER+/PR-/HER2+	1+	2+	Low FGFR1, Moderate FGF2
36	IDC	II	ER+/PR-/HER2+	0	1+	Negative FGFR1, Low FGF2
37	Invasive Mammary	II	ER-/PR-/HER2-	3+	2+	High FGFR1, Moderate FGF2
38	IDC	II	ER-/PR-/HER2-	2+	1+	Moderate FGFR1, Low FGF2
39	Micropapillary	High	ER-/PR-/HER2-	1+	2+	Low FGFR1, Moderate FGF2
40	Invasive Mammary	III	ER+/PR-/HER2+	0	3+	Negative FGFR1, High FGF2
41	Invasive Mammary	High	ER+/PR+/HER2+	0	0	Negative FGFR1, Negative FGF2
42	Invasive Mammary	II	NR/NR/NR	0	1+	Negative FGFR1, Low FGF2
43	IDC	III	ER+/PR+/HER2-	0	2+	Negative FGFR1, Moderate FGF2
44	IDC	III	ER-/PR-/HER2-	3+	0	High FGFR1, Negative FGF2
45	Invasive Mammary	High	ER+/PR+/HER2+	2+	2+	Moderate FGFR1, Moderate FGF2
46	Invasive Mammary	II	ER+/PR-/HER2+	3+	2+	High FGFR1, Moderate FGF2
47	Invasive Mammary	II	ER-/PR-/HER2-	1+	3+	Low FGFR1, High FGF2
48	Invasive Mammary	II	NR/NR/NR	3+	2+	High FGFR1, Moderate FGF2
49	IDC	High	ER+/PR-/HER2+	1+	2+	Low FGFR1, Moderate FGF2
50	Invasive Mammary	II	ER+/PR-/HER2+	3+	2+	High FGFR1, Moderate FGF2
51	IDC	II	NR/NR/NR	1+	2+	Low FGFR1, Moderate FGF2
52	IDC	III	ER+/PR+/HER2-	0	2+	Negative FGFR1, Moderate FGF2
53	IDC	III	ER+/PR+/HER2-	3+	2+	High FGFR1, Moderate FGF2
54	IDC	II	ER-/PR-/HER2-	0	0	Negative FGFR1, Negative FGF2
55	Invasive Mammary	II	ER+/PR+/HER2-	2+	1+	Moderate FGFR1, Low FGF2
56	Invasive Mammary	II	NR/NR/NR	3+	2+	High FGFR1, Moderate FGF2
57	IDC	II	ER+/PR+/HER2+	1+	1+	Low FGFR1, Low FGF2
58	Micropapillary	III	ER+/PR+/HER2+	1+	0	Low FGFR1, Negative FGF2
59	Micropapillary	III	ER+/PR-/HER2+	1+	2+	Low FGFR1, Moderate FGF2
60	Micropapillary	III	NR/NR/NR	3+	3+	High FGFR1, High FGF2